ORIGINAL ARTICLE

JBMR®

Combined MEK Inhibition and BMP2 Treatment Promotes Osteoblast Differentiation and Bone Healing in *Nf1*$_{Osx}^{-/-}$ Mice

Jean de la Croix Ndong,[1,2] David M Stevens,[3,4] Guillaume Vignaux,[1,2] Sasidhar Uppuganti,[1,5] Daniel S Perrien,[1,5,6,7] Xiangli Yang,[1,2,4] Jeffry S Nyman,[1,5,6] Eva Harth,[3,7] and Florent Elefteriou[1,2,4,8]

[1]Vanderbilt Center for Bone Biology, Vanderbilt University Medical Center, Nashville, TN, USA
[2]Department of Medicine, Vanderbilt University Medical Center, Nashville, TN, USA
[3]Department of Chemistry, Vanderbilt University Medical Center, Nashville, TN, USA
[4]Department of Pharmacology, Vanderbilt University Medical Center, Nashville, TN, USA
[5]Department of Orthopaedic Surgery and Rehabilitation, Vanderbilt University Medical Center, Nashville, TN, USA
[6]Department of Veterans Affairs, Tennessee Valley Healthcare System, Nashville, TN, USA
[7]Vanderbilt University Institute of Imaging Sciences, Vanderbilt University Medical Center, Nashville, TN, USA
[8]Department of Cancer Biology, Vanderbilt University Medical Center, Nashville, TN, USA

ABSTRACT

Neurofibromatosis type I (NF1) is an autosomal dominant disease with an incidence of 1/3000, caused by mutations in the *NF1* gene, which encodes the RAS/GTPase-activating protein neurofibromin. Non-bone union after fracture (pseudarthrosis) in children with NF1 remains a challenging orthopedic condition to treat. Recent progress in understanding the biology of neurofibromin suggested that NF1 pseudarthrosis stems primarily from defects in the bone mesenchymal lineage and hypersensitivity of hematopoietic cells to TGFβ. However, clinically relevant pharmacological approaches to augment bone union in these patients remain limited. In this study, we report the generation of a novel conditional mutant mouse line used to model NF1 pseudoarthrosis, in which *Nf1* can be ablated in an inducible fashion in osteoprogenitors of postnatal mice, thus circumventing the dwarfism associated with previous mouse models where *Nf1* is ablated in embryonic mesenchymal cell lineages. An ex vivo–based cell culture approach based on the use of *Nf1*$^{flox/flox}$ bone marrow stromal cells showed that loss of *Nf1* impairs osteoprogenitor cell differentiation in a cell-autonomous manner, independent of developmental growth plate–derived or paracrine/hormonal influences. In addition, in vitro gene expression and differentiation assays indicated that chronic ERK activation in *Nf1*-deficient osteoprogenitors blunts the pro-osteogenic property of BMP2, based on the observation that only combination treatment with BMP2 and MEK inhibition promoted the differentiation of *Nf1*-deficient osteoprogenitors. The in vivo preclinical relevance of these findings was confirmed by the improved bone healing and callus strength observed in *Nf1*$_{osx}^{-/-}$ mice receiving Trametinib (a MEK inhibitor) and BMP2 released locally at the fracture site via a novel nanoparticle and polyglycidol-based delivery method. Collectively, these results provide novel evidence for a cell-autonomous role of neurofibromin in osteoprogenitor cells and insights about a novel targeted approach for the treatment of NF1 pseudoarthrosis.

KEY WORDS: NEUROFIBROMATOSIS; GENETIC ANIMAL MODELS; PRECLINICAL STUDIES; BMPS; STROMAL/MESENCHYMAL STEM CELLS; OSTEOBLASTS; ANABOLICS

Introduction

Children and adults with neurofibromatosis type 1 (NF1; OMIM 162200) can present with a number of skeletal maladies. Osteopenia, idiopathic scoliosis, short stature, chest wall deformities and sphenoid wing dysplasia are amenable to acceptable clinical care.[1] In contrast, dystrophic scoliosis and long bone dysplasia represent two skeletal conditions associated with high morbidity, costs, and burden in these patients. Dystrophic scoliosis usually presents in pre-adolescents as sharp angulation over a short segment of the spine,[2] is frequently associated with paraspinal or other internal neurofibromas,[3,4] and is treated with often invasive surgeries in skeletally immature and growing children. Long bone dysplasia in infants with NF1 is usually unilateral and commonly involves the tibia. Dysplastic tibias frequently sustain fracture with minimum trauma, followed by non-union (pseudoarthrosis). Bracing techniques are used to reduce chances of fracture until children reach skeletal maturity.

Received in original form March 30, 2014; revised form June 19, 2014; accepted July 8, 2014. Accepted manuscript online July 17, 2014
Address correspondence to: Florent Elefteriou, PhD, Vanderbilt University Medical Center, 2215 Garland Avenue, Light Hall, Room 1255D, Nashville, TN 37232-0575, USA. E-mail: florent.elefteriou@vanderbilt.edu
Additional Supporting Information may be found in the online version of this article.

Journal of Bone and Mineral Research, Vol. 30, No. 1, January 2015, pp 55–63
DOI: 10.1002/jbmr.2316

Invasive and repetitive surgeries make this condition a challenging one to treat and often lead to amputation. Knowledge about natural history and pathogenesis of the NF1 skeletal maladies is still speculative, contributing to the lack of consensus regarding treatments.

The identification of effective drug targets to promote osteoblast differentiation and eventually bone union in individuals with NF1 pseudarthrosis will require a better understanding of the molecular basis of the differentiation defect of *Nf1*-deficient bone cells. TGFβ signaling inhibition has recently been shown to improve bone mass and bone healing in a model of NF1 skeletal defects;[5] however, it remains to be addressed whether TGFβ signaling is increased in human NF1 dysplastic bones. On the other hand, the use of rBMP2 to promote bone repair in individuals with NF1 pseudarthrosis and in related preclinical mouse models has had limited success,[6–10] leading us to test the hypothesis that *Nf1* deficiency in osteoprogenitors may impair BMP2 signaling and its bone anabolic properties. In this study, we created a new mouse model characterized by *Nf1* deficiency in postnatal mesenchymal bone progenitors to determine the potential of MEK inhibition by Trametinib, a MEK inhibitor currently in phase III clinical studies, to increase BMP2 efficacy in promoting bone healing.

Materials and Methods

Animals

All procedures were approved by the Institutional Animal Care and Use Committee (IACUC) at Vanderbilt University Medical Center. WT and $Nf1_{TetOff\text{-}Osx}{}^{-/-}$ mice (herein called $Nf1_{Osx}{}^{-/-}$ mice) were generated by crossing $Nf1^{flox/flox}$ mice[11] and *Osx*-tTA, *tetO*-cre;$Nf1^{flox/flox}$mice.[12] To repress transactivation of Cre by the *Osx* promoter during development, 200 μg/mL doxycycline was added to the drinking water of pregnant mothers and pups and refreshed every 2 to 3 days, until the time at which recombination/deletion of *Nf1* was desired. All experimental mice were originated from the same colony to increase genetic homogeneity.

For genotyping, genomic DNA was isolated from tail snips by sodium hydroxide digestion, and PCR was performed using primers P1, P2, and P4, as described by Zhu and colleagues.[11] The *Osx-Cre* transgene was detected using the forward: 5′-GCG GTC TGG CAG TAA AAA CTA TC-3′ and reverse: 5′-GTG AAA CAG CAT TGC TGT CAC TT-3′ primers.

Generation of mid-diaphyseal fractures

Closed mid-diaphyseal fracture of the tibia was created by three-point bending with an Einhorn device in 2-month-old male and female mice, as previously described.[13] To produce stabilized fractures, an intramedullary fixation was used by inserting a 0.25-mm metal insect pin in the tibial tuberosity through the patellar tendon before the creation of the fracture. Buprenorphine was administered subcutaneously for pain control. X-rays were taken after fracture to exclude any mice with unsatisfactory fractures.

Cell culture

Bone marrow stromal cells (BMSCs) were extracted from long bones by centrifugation of dissected femoral and tibial diaphyses at 2000*g* for 3 minutes. The cells were then counted, plated, and grown for 7 days in α-MEM supplemented with 10% fetal bovine serum (FBS), 100 IU/mL penicillin, 100 μg/mL streptomycin (Cellgro, Manassas, VA, USA). At day 7, mineralization was induced by the addition of 50 μg/mL of ascorbic acid and 10 mM β-glycerophosphate. The media was refreshed every 2 to 3 days for 10 more days.

Gene expression assays

Total RNA was extracted using TRIzol (Invitrogen, Grand Island, NY, USA), and cDNAs were synthesized after DNase I treatment using the high-capacity cDNA reverse-transcription kit (Applied Biosystems, Carlsbad, CA, USA). Quantitative (qPCR) was performed by using TaqMan or SYBR green gene expression assays. The probe and primer sets for *Runx2* (Mm00501578_m1), *CyclinD* (Mm00432359_m1), *Osx* (Mm00504574_m1), *Tnsap* (Mm00475834_m1), and the normalizer *Hprt* (Mm00446968_m1) were obtained from Applied Biosystems. The SYBR green primers were: *Nf1* (forward: GTATTGAATTGAAGCACCTTTGTTTGG; reverse: CTGCCCAAGGC-TCCCCCAG); *Ocn* (forward: ACCCTGGCTGCGCTCTGTCTCT; reverse: GATGCGTTTGTAGGCGGTCTTCA); and *Col1a1* (forward: GACATCCCTGAAGTCAGCTGC; reverse: TCCCTTGGGTCCCTCGAC). Specificity of amplification was verified by the presence of a single peak on the dissociation curve. Specific amplification conditions are available upon request. Measurements were performed in triplicate and from at least three independent experiments.

Western blot analyses

Whole-cell lysates were separated by SDS-PAGE electrophoresis according to standard protocols. Nitrocellulose membranes were probed using standard protocols using an anti-Phospho-ERK1/2 antibody (Cell Signaling, Danvers, MA, USA; cat# 9101, dilution 1:1000) and an anti-ERK1/2 antibody (Cell Signaling cat# 9102, dilution 1:1000).

Cell culture staining

Tissue nonspecific alkaline phosphatase (TNSALP) activity was assayed using an ALP assay kit (Sigma, St. Louis, MO, USA). Cell supernatant or lysate from adherent cells plated in 12-well plates were incubated with 20 mM p-nitrophenylphosphate in reaction buffer (50 mM Tris-HCl, pH 8.8, 10 mM $MgCl_2$) for 5 to 10 minutes at 37°C, then the reaction was stopped with 0.1 N NaOH, and the absorbance was read at 405 nm.

For Alizarin staining, cells in 12-well plates were washed twice in 1× PBS and stained with a solution containing 40 mM Alizarin red S solution. The plates were incubated at room temperature for 20 minutes, then washed and air-dried. Bound calcium was released by adding 1 mL of acetic acid, and the mixture was incubated for 20 minutes. One hundred microliters of the solution was collected for OD_{405} measurement.

Adenovirus infection of BMSCs

BMSCs were isolated from $Nf1^{flox/flox}$ mice and seeded at a density of 10^6 cells/well in 12-well plates. At 40% confluence, cells were incubated in complete cell culture medium (α-MEM, 10% FBS and 100 IU/mL penicillin) containing either Ad5-CMV-GFP or Ad5-CMV-cre (Vector Development Lab, Baylor College of Medicine, Houston, TX, USA) at 2.5×10^9 PFUs. After 2 days of incubation, the medium in each well was replaced with complete cell culture medium. *Nf1* mRNA and recombination efficiency were determined according to the protocol previously described by Wang and colleagues.[14]

Polyester nanoparticle synthesis (NP)

Poly(α-allyl-valerolactone, valerolactone) containing 4% allyl groups was epoxidized with meta-chloroperoxybenzoic acid (mcpba, 1.2 eq per alkene, Sigma) in CH_2Cl_2 (0.065 M alkene) for 48 hours and washed with saturated sodium bicarbonate.[15] The resulting polymer was dried under reduced pressure. 2,2′-ethylenedioxy-bis(ethylamine) (7.5 μL, 0.51 mmol, Sigma) was added to a solution of poly(epoxide-valerolactone, valerolactone) (0.173 g, $M_n = 3{,}644$ Da) dissolved in CH_2Cl_2 (21.1 mL). The reaction mixture refluxed for 12 hours at 46°C. Residual bisamine was removed by dialyzing with Snakeskin Pleated Dialysis Tubing (MWCO = 10,000) against CH_2Cl_2 to yield nanoparticles (NP).

Trametinib encapsulation into nanoparticles

A solution of nanoparticle (23.0 mg) and MEK inhibitor (Trametinib, 5.0 mg, GlaxoSmithKline, Brentford, UK) in DMSO (1.00 mL) was added drop-wise to a vortexing solution of aqueous 1% d-α-tocopherolpolyethyleneglycol (1000) succinate (Vit E-TPGS [Sigma], 14.0 mL). The resulting precipitate was washed with deionized water using three cycles of centrifugation at 7830 rpm for 20 minutes. The precipitate was freeze-dried to yield a white powder (6.4% MEK inhibitor/NP [wt/wt] determined by NanoDrop UV-Vis at 258 nm).

Polyglycidol-BMP2/NP-Trametinib dual drug delivery system

Polyglycidol homopolymer[16] was synthesized by first stirring 3-methyl-1-butanol (0.98 mL, 1.7 M in anhydrous THF) with $Sn(OTf)_2$ (1.28 mL, 0.037 M in anhydrous THF) in a nitrogen-purged flask. Glycidol monomer (10.0 g, 135 mmol, Sigma) was added drop-wise to the cooled reaction mixture. After the monomer addition was complete, the reaction vessel was allowed to warm up to room temperature. Once stirring was completely impeded, the crude viscous polymer product was dissolved in a minimal amount of methanol and precipitated into vigorously stirring acetone, which was then decanted to afford the pure glycidol homopolymer product as a translucent, viscous material. Recombinant human bone morphogenic protein-2 (rBMP2, Creative Biomart, Shirley, NY, USA) was suspended in 20 mM acetic acid (10 mg/mL), added to polyglycidol, and diluted with PBS for a rBMP2 concentration of 0.50 μg/μL[6] and polyglycidol concentration of 0.46 g/mL.

For Trametinib injections and combo injections, encapsulated Trametinib was first sonicated in PBS and transferred to the polyglycidol mix to yield a Trametinib concentration of 0.188 μg/μL.[17,18] Vehicle was prepared using unloaded nanoparticles and formulated similarly as described above.

X-rays and micro-computed tomography (μCT) analyses

Radiographs were obtained using a digital cabinet X-ray system (LX-60, Faxitron, Tucson, AZ, USA). μCT analyses were performed using a high-resolution benchtop Scanco μCT 40 system (Scanco Medical, Bassersdorf, Switzerland). Tomographic images were acquired at 55 kVp and 145 mA with an isotropic voxel size of 12 μm and at an integration time of 250 ms with 1000 projections collected per 360° rotation. Scans were acquired in PBS. μCT images were reconstructed, filtered ($\sigma = 0.8$ and support = 1.0) and thresholded at 200. Callus trabecular bone was contoured manually on every 10 sections, and sections in between were automatically contoured with the software algorithm.

Biomechanical testing

The fractured tibia from wild-type (WT) and $Nf1_{Osx}^{-/-}$ littermates was cleaned of soft tissue and stored frozen in PBS until thawed for testing. Three-point-bending was accomplished in displacement control on an Instron DynaMight 4481 servo-hydraulic material testing apparatus (Instron, Norwood, MA, USA). Hydrated samples were tested with span of 6 mm at a rate of 3 mm/min as per Tan and colleagues.[19] Force was measured using a 100 N load cell, and displacement was measured by a linear variable displacement transducer. Structural properties were extracted from force-displacement curves by custom Matlab algorithms (Mathworks, Natick, MA, USA).

Statistical analyses

A one-way analysis of variance (ANOVA) was used to determine whether differences existed in μCT and biomechanical-derived properties among experimental groups. In the event that standard deviations were significantly different, the ANOVA was done by the nonparametric Kruskal-Wallis test. When differences existed at $p < 0.05$, post hoc, pair-wise comparisons were tested for significance in which the p value was adjusted ($p_{adj} < 0.05$) by Holm-Sidak's method or Dunn's method (nonparametric). Statistical analysis was performed using GraphPad PRISM (v6.0a, La Jolla, CA, USA). Data are provided as mean ± SD.

Results

Growth plate–independent and cell-autonomous differentiation defect in *Nf1*-deficient osteoprogenitors

Conditional deletion of *Nf1* early in the mesenchymal lineage, using the *Col2a1*- or *Prx*-cre transgenic promoters,[14,20,21] triggered skeletal phenotypes in mice that phenocopy structural and cellular deficits observed in human NF1 skeletal lesions, including low bone mass, hyperosteoidosis (accumulation of nonmineralized bone matrix), increased osteoclastogenesis, and delayed bone healing. However, the noninducible nature of these promoter constructs resulted in *Nf1* deficiency in growth plate chondrocytes during development, leading to pups born with a reduced stature and thus complicating the interpretation of the cellular cause of the bone phenotypes observed because growth plate defects impact bone development, bone accrual, and osteoblast differentiation.[21,22] To determine if loss of *Nf1* function in osteoblast progenitors impairs their differentiation in vivo, independently of developmental growth plate osteochondroprogenitors or secreted factors, we generated a new mouse model that lacks *Nf1* in postnatal *Osterix* (*Osx*)-positive osteoprogenitors ($Nf1_{osx}^{-/-}$ mice). This model was generated by crossing mice with *Nf1* floxed alleles[11] and mice expressing the cre-recombinase under the control of the Osterix (*Osx* or *Sp7*) promoter, which can be regulated by a doxycycline-dependent on/off switch (Tet^{off} system).[12] Our breeding strategy generated 50% of $Nf1^{flox/flox}$; cre-negative (WT) and 50% of $Nf1^{flox/flox}$;cre-positive ($Nf1_{osx}^{-/-}$) littermates. In absence of doxycycline treatment, these mutant mice exhibited reduced stature owing to *Osx*-cre activity in chondrocytes during development[23,24] but were born with a normal size and did not show a short stature phenotype in adults when given doxycycline (doxy) from conception to 2 weeks of age to repress cre activity and to prevent *Nf1* recombination during development (Fig. 1*A*). To assess the differentiation properties of *Nf1*-deficient osteoprogenitors, BMSCs were isolated from 2-month-old WT and $Nf1_{osx}^{-/-}$

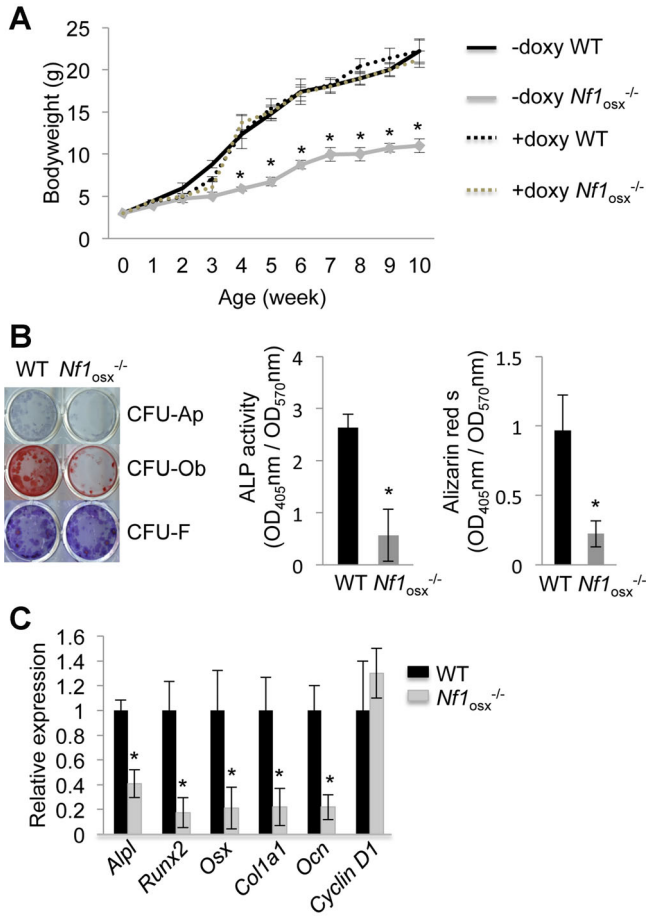

Fig. 1. Differentiation and gene expression changes induced by *Nf1* loss of function in osteoprogenitor cells. (*A*) Doxycycline (Doxy) administration corrects the growth retardation of $Nf1_{Osx}^{-/-}$ mice. Doxy was given from conception to up to 10 weeks of age. (*B*, *C*) Differentiation assays. BMSCs isolated from WT and $Nf1_{osx}^{-/-}$ mice were cultured for 2 weeks in osteogenic conditions. BMSC differentiation was analyzed by alkaline phosphatase (ALP) staining (differentiation, CFU-Ap), Alizarin red-S staining (mineralization, CFU-Ob), and crystal violet staining (cell number, CFU-F). In identical cultures, gene expression was assessed by qPCR. The results represent the mean ± SD and are representative of triplicate experiments. $^{*}p < 0.05$ versus WT.

mice (treated by doxy from conception to 2 weeks of age), and the number of CFU-Ap and CFU-Ob colonies were quantified as an indirect measure of the in vivo number of bone osteoprogenitors. BMSCs from $Nf1_{osx}^{-/-}$ mice formed significantly fewer CFU-Ap and CFU-Ob colonies than BMSCs from WT littermates (Fig. 1*B*) and were characterized by a significant decrease in the expression of major osteoblast marker genes, including *Alpl, Runx2, Osx, Col1a1*, and *Ocn* compared with WT BMSCs, as quantified by qPCR analyses (Fig. 1*C*). These results indicate that the bones of $Nf1_{osx}^{-/-}$ mice contain a reduced number of osteoprogenitors, in line with their low bone mass, cortical bone thinning, and weakened mechanical properties,[25] and suggest that the impaired differentiation of *Nf1*-deficient osteoprogenitors is growth plate independent.

To determine whether the differentiation defect of $Nf1^{-/-}$ osteoprogenitors is indeed growth plate independent and cell autonomous, we used BMSCs isolated from $Nf1^{flox/flox}$ mice,[11] infected ex vivo with GFP- or Cre-expressing adenoviruses. This approach allowed us to avoid any bias from in vivo–derived factors or conditions that could affect the early commitment, proliferation, or differentiation of *Nf1*-deficient osteoprogenitors and to start the differentiation assays in cultures plated at the same density and same differentiation stage. BMSCs from long bones of $Nf1^{flox/flox}$ mice were isolated, cultured for 7 days in normal medium, and infected with a GFP- (Ad-CMV-GFP, control) or Cre-adenovirus (Ad-CMV-Cre). This approach led to an approximate 70% recombination efficiency, as shown by genomic PCR (Fig. 2*A*) and RT-PCR for *Nf1* expression (Fig. 2*B*). After adenoviral infection, BMSCs were induced to differentiate by supplementation of the culture medium with ascorbic acid and glycerophosphate. Differentiation CFU assays revealed that ex vivo *Nf1* ablation in $Nf1^{flox/flox}$ BMSCs induces a significant reduction in the number of CFU-Ap and CFU-Ob colonies after 14 days of differentiation (Fig. 2*C, D*). These results, consistent with studies using alternative models,[26,27] indicate that neurofibromin, independently from growth plate, bone marrow, or systemic influences, is required for normal osteoprogenitor cell differentiation and matrix mineralization.

An ERK-dependent blunted response to BMP2 contributes to the defective differentiation of $Nf1^{-/-}$ osteoblasts

BMPs are well known for their osteogenic properties and are clinically used in the management of skeletal conditions requiring bone anabolism. However, recombinant BMP2 failed

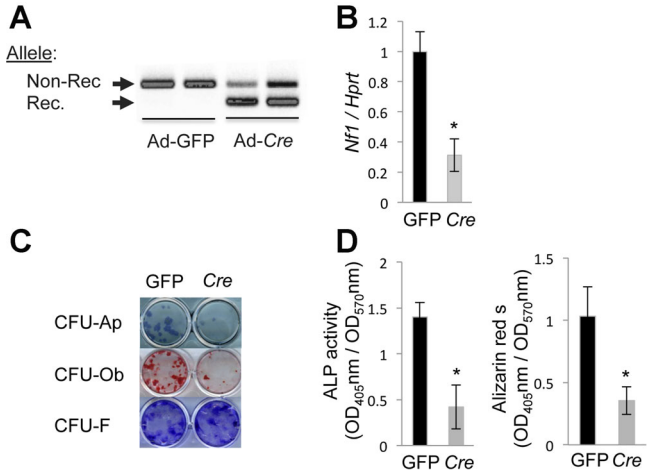

Fig. 2. *Nf1* loss of function in osteoprogenitor cells impairs differentiation independently of growth plate and systemic abnormalities. (*A, B*) BMSCs isolated from $Nf1^{flox/flox}$ mice were infected in vitro with a GFP- (control) or cre-adenovirus (Ad), and cultures were differentiated for 14 days in osteogenic conditions. (*A*) Non-recombined (Non-Rec.) and recombined (Rec.) *Nf1* alleles detected by PCR using genomic DNA from primary cells. (*B*) *Nf1* expression analyzed by qPCR and normalized by *Hprt*. (*C*) BMSC differentiation was analyzed by ALP staining (differentiation, CFU-Ap), Alizarin red-S staining (mineralization, CFU-Ob), and crystal violet staining (cell number, CFU-F). (*D*) Quantification of ALP activity (OD_{405}) and released Alizarin red-S (OD_{405}), normalized by cell number (OD_{570}) in the same cultures. The results represent the mean ± SD and are representative of triplicate experiments. $^{*}p < 0.05$ versus WT.

to promote osteoblast differentiation and bone healing in two NF1 mouse models.[6,7] These results suggested reduced *Bmp2* expression was unlikely to cause the differentiation phenotype of *Nf1*-deficient osteoprogenitors. Because a common trait of *Nf1*-deficient cells, including osteoblasts, is constitutive activation of the RAS-ERK pathway, we hypothesized that chronic/ uncontrolled activation of RAS-ERK signaling in $Nf1^{-/-}$ osteoprogenitors could antagonize the osteogenic properties of BMP2 and explain the reduced differentiation potential of these cells. To address this hypothesis, BMSCs were prepared from 2-month-old WT and $Nf1_{osx}^{-/-}$ mice (treated by doxy from conception to 2 weeks of age) and were differentiated in osteogenic conditions for 14 days in vitro, in the presence of vehicle (DMSO), rhBMP2 (100 ng), and the MEK inhibitor Trametinib (0.1 μM), alone or in combination with BMP2. In these cultures, a higher level of P-ERK was detected in BMSCs prepared from $Nf1_{osx}^{-/-}$ mice compared with WT mice (Fig. 3*A*), and Trametinib potently abolished ERK1/2 phosphorylation, with or without BMP2

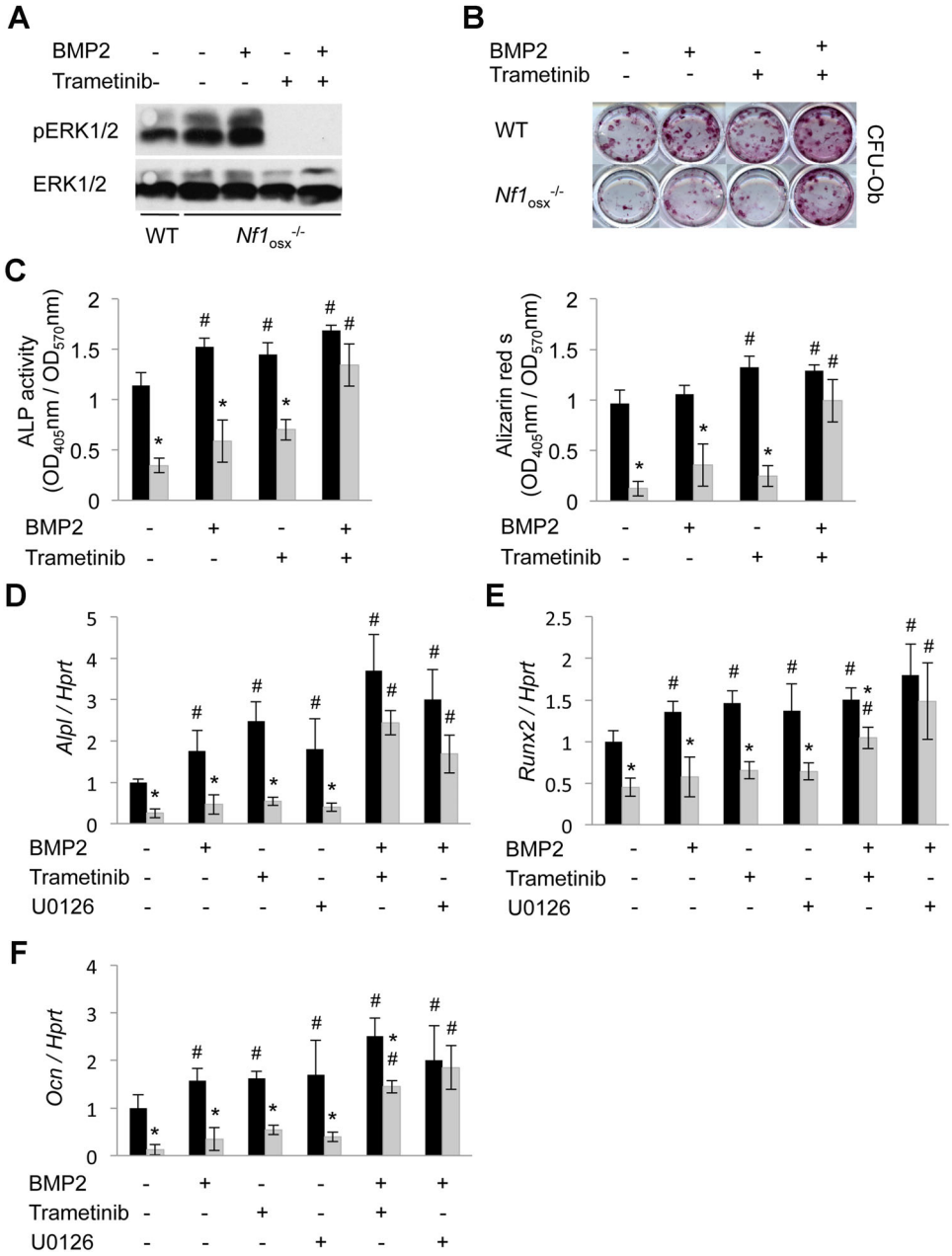

Fig. 3. Combination treatment with BMP2 and Trametinib corrects the differentiation defect of $Nf1^{-/-}$ osteoprogenitors. (*A*) BMSCs isolated from WT and $Nf1_{osx}^{-/-}$ mice were serum-starved overnight and then preincubated with Trametinib (0.1 μM) for 30 minutes. BMP2 (100 ng) treatment was started 30 minutes later for 1 hour. Whole BMSC lysates were separated by SDS/PAGE and immunoblotted using the indicated antibodies. (*B, C*) BMSCs isolated from WT and $Nf1_{osx}^{-/-}$ mice were treated with vehicle (DMSO), BMP2 (100 ng/mL), Trametinib (0.1 μM), or both drugs for 2 weeks, and BMSC differentiation was analyzed by Alizarin red-S (CFU-Ob, *B*) and ALP activity (*C*). (*D–F*) Similar cultures were treated with vehicle (DMSO), BMP2 (100 ng/mL), the MEK inhibitors U0126 (1 μM) or Trametinib (0.1 μM), or combined BMP2/U0126 or BMP2/Trametinib for 2 weeks. Expression of osteoblast marker genes was assessed by qPCR ($n = 3$). Black bars = WT mice; gray bars = $Nf1_{Osx}^{-/-}$ mice. $^{*}p < 0.05$ versus WT; $\#p < 0.05$ versus nontreated in the same genotype group.

treatment. Osteogenic differentiation assays showed that rBMP2 treatment increased the number of CFU-Ob colonies in BMSC cultures from WT mice, as expected, but failed to do so in *Nf1*-deficient BMSCs (Fig. 3*B, C*). Consistent with previous data in WT osteoblasts,[28,29] MEK inhibition enhanced differentiation of WT BMSCs but had no effect on the differentiation of *Nf1*-deficient BMSCs either. However, combination treatment with Trametinib and rBMP2 significantly increased the number of CFU-Ob colonies in *Nf1*-deficient BMSC cultures (Fig. 3*B, C*) and resulted in an increase in osteoblast marker gene expression, including *Alpl, Runx2*, and *Ocn* (Fig. 3*D–F*). Similar results were obtained with U0126, a commonly used MEK inhibitor.[25] These results indicate that controlled RAS/ERK signaling is required for the proper response of osteoprogenitors to BMP2 and suggest that Trametinib and BMP2 treatment may have beneficial effects in the setting of NF1 skeletal maladies.

Nf1 loss of function in callus osteoprogenitor cells impairs bone healing

The inducible nature of the $Nf1_{osx}^{-/-}$ mouse model allows one to ablate *Nf1* in a controlled manner in periosteal and bone marrow osteoprogenitors in adult mice (hence, circumventing developmental phenotypes) and at selected times during the bone-healing process after fracture by simply stopping doxy treatment. To determine the contribution of defective *Nf1*-deficient osteoprogenitors and their lineage-derived cells to bone healing in mice that do not exhibit the reduced stature characteristic of the *Col2a1*-cre- and *Prx*-cre-driven *Nf1*-deficient mice,[14,21,30] we administered doxy to pregnant mothers and their pups from conception to 2 weeks of age to repress cre expression during growth, after which doxy treatment was stopped and a closed tibia fracture was generated at 2 months of age, as described previously.[13] Doxy removal from the drinking water led to a 20% to 40% recombination efficiency of the *Nf1* floxed alleles (Fig. 4*A*) and to a 60% reduction in *Nf1* expression (Fig. 4*B*) in total bone lysates, which is consistent with the complex cellularity of the bone marrow and restricted cre-driven gene recombination in osteoprogenitor cells. High-resolution X-ray analyses revealed that callus formation was severely impaired in $Nf1_{osx}^{-/-}$ mice compared with WT mice, as visualized by the formation of an atrophic callus 21 days post-fracture (Fig. 4*C*). Three-dimensional microtomographic analyses confirmed the existence of a significantly smaller calcified callus 21 day post-fracture (callus tissue volume, Fig. 4*D*), despite normal bone shaft cross-sectional tissue area, Fig. 4*E*), as well as a lower callus tissue mineral density (TMD, Fig. 4*F*) and callus BV/TV (Fig. 4*G*) in $Nf1_{osx}^{-/-}$ mice compared with WT mice. Most significantly, three-point bending tests indicated that calluses from $Nf1_{osx}^{-/-}$ mice were less stiff and mechanically weaker than the ones from WT mice, as measured by flexural testing (Fig. 4*H, I*). These results indicate that *Nf1* loss of function in postnatal osteoprogenitors has significant in vivo deleterious repercussions on the bone-healing process and establish the $Nf1_{osx}^{-/-}$ mouse model as a useful tool to investigate the etiology of NF1 pseudarthrosis and novel approaches to promote bone healing in NF1.

Local administration of Trametinib and BMP2 promotes bone healing in $Nf1_{Osx}^{-/-}$ mice

Based on the beneficial effect of Trametinib and BMP2 combination treatment on $Nf1^{-/-}$osteoprogenitor differentiation observed in vitro, we asked whether such treatment could promote bone healing and improve callus bone parameters in

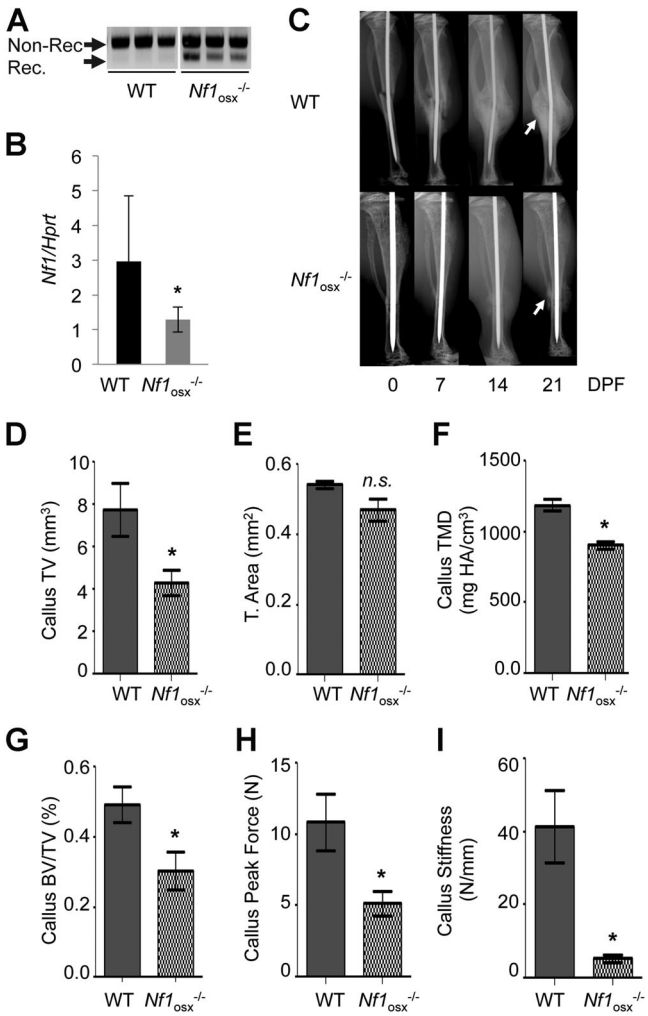

Fig. 4. *Nf1* loss of function in osteoblasts delays bone healing in $Nf1_{osx}^{-/-}$ mice. (*A*) Genomic DNA was extracted from tibias of 2-month-old mice. *Nf1* genomic recombination was evaluated by PCR to detect nonrecombined (Non-Rec.) and recombined (Rec.) *Nf1* alleles ($n = 3$). (*B*) *Nf1* expression in tibias from 2-month-old mice was measured by qPCR ($n = 6$). (*C*) WT and $Nf1_{Osx}^{-/-}$ mice were subjected to tibia fracture, and callus X-ray analyses were performed 7, 14, and 21 days post-fracture (DPF). (*D–G*) 3D μCT quantification of callus tissue volume (TV) (*D*), bone cross-sectional tissue area (*E*), callus tissue mineral density (TMD) (*F*), and callus bone volume over total volume (BV/TV) (*G*) in WT and $Nf1_{Osx}^{-/-}$ mice 21 DPF. (*H, I*) Callus strength (maximum force) (*H*) and callus stiffness (*F*) measured by three-point bending tests in WT and $Nf1_{Osx}^{-/-}$ 21 DPF ($n = 10$ to 15 mice/group). $^{*}p < 0.05$. ns = nonsignificant.

$Nf1_{osx}^{-/-}$ mice. Because of the hydrophobic nature of Trametinib, we generated a drug delivery system based on polyester nanoparticles that allow progressive release of Trametinib at the fracture site. Using a 4% cross-linking density, the in vitro release of Paclitaxel (a BCS class IV hydrophobic drug like Trametinib) was continuous and reached 50% within a 10-day period at 37°C, pH 7.4 (Supplemental Fig. S1 and Harth and colleagues).[31] In addition, we used a polyglycidol-based delivery method to limit the diffusion of BMP2 and Trametinib-loaded nanoparticles

at the injection site. WT and $Nf1_{osx}^{-/-}$ mice were subjected to tibia fracture after doxy withdrawal, as described above. At days 1 and 7 post-fracture, mice were injected at the fracture site with 20 μL vehicle (nanoparticles and PEG), 20 μL rBMP2-polyglycidol (0.50 μg/μL), 20 μL Trametinib nanoparticles (0.188 μg/μL), or 20 μL of both (Fig. 5*A*). In the latter group, Trametinib nanoparticles were dispersed in the polyglycidol-based delivery system containing rBMP2. Consistent with the in vitro results, rBMP2 and Trametinib treatment alone did not improve bone-healing parameters in $Nf1_{osx}^{-/-}$ mice (Fig. 5*B–F*), whereas callus TV, BV, BV/TV, and TMD were significantly higher in $Nf1_{osx}^{-/-}$ mice treated with the rBMP2+Trametinib combination compared with vehicle or single drug controls (Fig. 5*B–F*). In addition, mice treated with BMP2+Trametinib had a callus with higher strength compared with mice treated with BMP2 or Trametinib alone, as indicated by their increased stiffness and peak force measured by three-point bending (Fig. 5*G*, *H*). From these findings, we conclude that MEK inhibition by Trametinib potentiates BMP2 efficacy in promoting bone healing in the context of *Nf1* deficiency in osteoprogenitor cells.

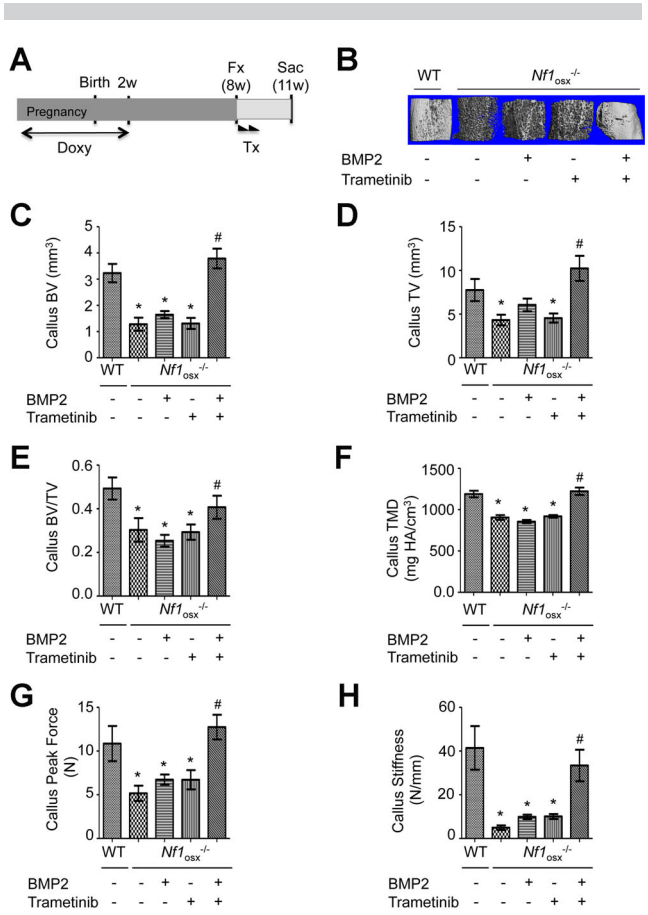

Fig. 5. Combined BMP2 treatment and MEK improves bone healing in $Nf1_{osx}^{-/-}$ mice. (*A–G*) After tibia fracture, WT and *Nf1osx*$^{-/-}$ mice were treated (Tx) with vehicle (nanoparticles and polyglycidol) or rBMP2-polyglycidol or Trametinib nanoparticles or both, 1 and 7 days post-fracture. (*A*) Treatment scheme. (*B–F*) 3D μCT representative reconstruction images (*B*), quantification of callus bone volume (BV) (*C*), callus tissue volume (TV) (*D*), callus bone volume over total volume (BV/TV) (*E*), and callus tissue mineral density (TMD) (*F*) in WT and $Nf1_{osx}^{-/-}$ mice 21 days post-fracture (DPF). (*G*, *H*) Callus strength (maximum peak force) (*G*) and callus stiffness (*H*) measured by three-point bending tests were significantly lower in $Nf1_{Osx}^{-/-}$ mice compared with WT mice, 21 DPF. $^{*}p < 0.05$ versus WT; $\#p < 0.05$ versus single treatment in the $Nf1_{Osx}^{-/-}$ mouse group ($n = 10$ to 15 mice/group).

Discussion

The clinical management of NF1 pseudarthrosis is challenging. This reflects the current poor understanding of the underlying pathophysiology of this condition and its variability among individuals with NF1. In this study, we show that lack of *Nf1* in osteoprogenitors, in a cell-autonomous fashion and independently from growth plate developmental alterations, is sufficient to impair their differentiation into mature osteoblasts and that the response of osteoprogenitors to BMP2 requires regulation of RAS/ERK signaling by neurofibromin. We also show that BMP2 can only promote bone healing in mice lacking *Nf1* in adult osteoprogenitors when the constitutive activation of RAS/ERK signaling typical of *Nf1*-deficient cells is suppressed.

These results differ from the ones from a previous study by Sharma and colleagues, which describes a beneficial effect the MEK inhibitor PD98059 in a mouse model of NF1-impaired healing, without the need of combined BMP2 treatment.[32] Apart from dosing considerations, the main difference between the two studies is the differentiation stage at which *Nf1* is ablated to generate *Nf1*-deficient bone cells. The use of the 2.3-kb *Col1a1*-cre mice to prepare *Nf1*-deficient BMSC cultures in the first study leads to *Nf1* deletion very specifically in osteoblasts, but in committed mature osteoblasts, whereas the *Osx*-cre and ex vivo adeno-cre approaches used in the current study lead to *Nf1* deletion in proliferative osteoprogenitor cells, which more closely reflects what occurs in individuals with NF1 pseudarthrosis. It is thus possible that the response of undifferentiated BMSCs to MEK inhibition and BMP2 is distinct from the one of committed *Col1a1*-positive osteoblasts and that the effects found in the model using the 2.3-kb *Col1a1*-cre mice are in fact caused by the rescue of other defects associated with *Nf1* loss of function and ERK activation, such as altered mineralization, collagen synthesis, and osteoclastogenesis, rather than differentiation.[25,32] In any case, our study indicates that *Nf1*-deficient osteoprogenitors display a blunted response to the osteogenic property of BMP2, which may directly contribute to the bone repair defect observed in $Nf1_{osx}^{-/-}$ mice. The beneficial effect of BMP2 combined with MEK inhibition in this model supports such a contribution that may coexist with the previously reported increase in hyperactive TGFβ signaling.[5] The relative contribution of these two mechanisms to the delay in bone healing observed in the NF1 setting will require further investigations, as both can independently modulate in vivo bone repair.[33–35]

Despite its well-recognized osteogenic properties, BMP2/7 was inefficient, on its own, in promoting bone union in patients with NF1 pseudarthrosis and in a mouse model of NF1 pseudarthrosis. Only a combination treatment with BMP2 and bisphosphonates was associated with better outcomes in mice and in a study assessing fracture union in 7 patients with NF1 pseudarthrosis.[6,7,36] The current study shows that BMP2 and MEK inhibition are both required to improve bone-healing parameters in mice lacking *Nf1* in osteoprogenitors. Although it is difficult to compare treatment efficacy in independent studies using different mouse models and drugs, these results point to the necessity of a dual treatment to significantly improve bone healing in the context of NF1 pseudarthrosis, reflecting the

multitude and complexity of molecular and cellular processes affected by *Nf1* loss of function.

In summary, this study revealed a blunted BMP2 response as a cause of the defective differentiation of *Nf1*-deficient osteoprogenitors and led to preclinical data supporting the use of a novel targeted combination therapy based on MEK inhibition (Trametinib) and rhBMP2 to promote bone healing in individuals with NF1 pseudarthrosis. Trametinib is FDA-approved for the treatment of patients with unresectable or metastatic melanoma with BRAF mutations. Hence, its use in the NF1 setting could have an advantage over the development of other drugs.

Disclosures

All authors state that they have no conflicts of interest.

Acknowledgments

This work was funded by a Young Investigator Award (2012-01-028) from the Children's Tumor Foundation (JN) and by the National Institute of Arthritis and Musculoskeletal and Skin Diseases, part of the National Institutes of Health, under Award Number 5R01 AR055966 (FE). Support for the micro–computed tomography equipment was provided by the National Institutes of Health, Award Number S10 RR027631 (DSP). Support for chemical synthesis was provided by the Department of Chemistry (EH).

Authors' roles: Study design: JDLCN and FE. Study conduct: JDLCN and FE. Data collection: JDLCN, DMS, GV, and SU. Data analysis: JDLCN, JSN, DSP, and FE. Data interpretation: JDLCN and FE. Drafting manuscript: JDLCN, XY, DMF and FE. Approving final version of manuscript: JDLCN, DMS, GV, SU, DSP, JSN, XY, EH, and FE. FE takes responsibility for the integrity of the data analysis.

References

1. Stevenson DA, Little D, Armstrong L, et al. Approaches to treating NF1 tibial pseudarthrosis: consensus from the Children's Tumor Foundation NF1 Bone Abnormalities Consortium. J Pediatr Orthop. 2013; 33(3):269–75.
2. Crawford AH, Herrera-Soto J. Scoliosis associated with neurofibromatosis. Orthop Clin North Am. 2007;38(4):553–62, vii.
3. Khong PL, Goh WH, Wong VC, Fung CW, Ooi GC. MR imaging of spinal tumors in children with neurofibromatosis 1. AJR Am J Roentgenol. 2003;180(2):413–7.
4. Ramachandran M, Tsirikos AI, Lee J, Saifuddin A. Whole-spine magnetic resonance imaging in patients with neurofibromatosis type 1 and spinal deformity. J Spinal Disord Tech. 2004;17(6):483–91.
5. Rhodes SD, Wu X, He Y, et al. Hyperactive transforming growth factor-beta1 signaling potentiates skeletal defects in a neurofibromatosis type 1 mouse model. J Bone Miner Res. 2013;28(12):2476–89.
6. Schindeler A, Ramachandran M, Godfrey C, et al. Modeling bone morphogenetic protein and bisphosphonate combination therapy in wild-type and Nf1 haploinsufficient mice. J Orthop Res. 2008;26(1): 65–74.
7. Schindeler A, Birke O, Yu NY, et al. Distal tibial fracture repair in a neurofibromatosis type 1-deficient mouse treated with recombinant bone morphogenetic protein and a bisphosphonate. J Bone Joint Surg Br. 2011;93(8):1134–9.
8. Anticevic D, Jelic M, Vukicevic S. Treatment of a congenital pseudarthrosis of the tibia by osteogenic protein-1 (bone morphogenetic protein-7): a case report. J Pediatr Orthop B. 2006;15(3): 220–1.
9. Lee FY, Sinicropi SM, Lee FS, Vitale MG, Roye DP Jr, Choi IH. Treatment of congenital pseudarthrosis of the tibia with recombinant human bone morphogenetic protein-7 (rhBMP-7). A report of five cases. J Bone Joint Surg Am. 2006;88(3):627–33.
10. Fabeck L, Ghafil D, Gerroudj M, Baillon R, Delince P. Bone morphogenetic protein 7 in the treatment of congenital pseudarthrosis of the tibia. J Bone Joint Surg Br. 2006;88(1):116–8.
11. Zhu Y, Romero MI, Ghosh P, et al. Ablation of NF1 function in neurons induces abnormal development of cerebral cortex and reactive gliosis in the brain. Genes Dev. 2001;15(7):859–76.
12. Rodda SJ, McMahon AP. Distinct roles for Hedgehog and canonical Wnt signaling in specification, differentiation and maintenance of osteoblast progenitors. Development. 2006;133(16):3231–44.
13. Wang W, Nyman JS, Moss HE, et al. Local low-dose lovastatin delivery improves the bone-healing defect caused by Nf1 loss of function in osteoblasts. J Bone Miner Res. 2010;25(7):1658–67.
14. Wang W, Nyman JS, Ono K, Stevenson DA, Yang X, Elefteriou F. Mice lacking Nf1 in osteochondroprogenitor cells display skeletal dysplasia similar to patients with neurofibromatosis type I. Hum Mol Genet. 2011;20(20):3910–24.
15. Stevens DM, Watson HA, LeBlanc MA, et al. Practical polymerization of functionalized lactones and carbonates with Sn(OTf)(2) in metal catalysed ring-opening polymerization methods. Polymer Chem. 2013;4(8):2470–4.
16. Spears BR, Waksal J, McQuade C, Lanier L, Harth E. Controlled branching of polyglycidol and formation of protein-glycidol bioconjugates via a graft-from approach with "PEG-like" arms. Chem Commun (Camb). 2013;49(24):2394–6.
17. Morris EJ, Jha S, Restaino CR, et al. Discovery of a novel ERK inhibitor with activity in models of acquired resistance to BRAF and MEK inhibitors. Cancer Discov. 2013;3(7):742–50.
18. Yamaguchi T, Kakefuda R, Tajima N, Sowa Y, Sakai T. Antitumor activities of JTP-74057 (GSK1120212), a novel MEK1/2 inhibitor, on colorectal cancer cell lines in vitro and in vivo. Int J Oncol. 2011; 39(1):23–31.
19. Tan AM, Tan CL, Phua KB, Joseph VT. Chemotherapy for hepatoblastoma in children. Ann Acad Med Singapore. 1990;19(2): 286–9.
20. Kolanczyk M, Kuhnisch J, Kossler N, et al. Modelling neurofibromatosis type 1 tibial dysplasia and its treatment with lovastatin. BMC Med. 2008;6:21.
21. Ono K, Karolak MR, Ndong JD, Wang W, Yang X, Elefteriou F. The Ras-GTPase activity of neurofibromin restrains ERK-dependent FGFR signaling during endochondral bone formation. Hum Mol Genet. 2013;22(15):3048–62.
22. Wang W, Lian N, Ma Y, et al. Chondrocytic Atf4 regulates osteoblast differentiation and function via Ihh. Development. 2012;139(3): 601–11.
23. Chen J, Shi Y, Regan J, Karuppaiah K, Ornitz DM, Long F. Osx-Cre targets multiple cell types besides osteoblast lineage in postnatal mice. PLoS One. 2014;9(1):e85161.
24. Maes C, Kobayashi T, Selig MK, et al. Osteoblast precursors, but not mature osteoblasts, move into developing and fractured bones along with invading blood vessels. Dev Cell. 2010;19(2):329–44.
25. Ndong J, Makowski AJ, Uppuganti S, et al. Asfotase-alpha improves bone growth, mineralization and strength in mouse models of neurofibromatosis type-1. Nat Med. 2014 Jul 6. PMID: 24997609.
26. Sharma R, Wu X, Rhodes SD, et al. Hyperactive Ras/MAPK signaling is critical for tibial nonunion fracture in neurofibromin-deficient mice. Hum Mol Genet. 2013;22(23):4818–28.
27. Leskela HV, Kuorilehto T, Risteli J, et al. Congenital pseudarthrosis of neurofibromatosis type 1: impaired osteoblast differentiation and function and altered NF1 gene expression. Bone. 2009;44(2):243–50.
28. Doan TKP, Park KS, Kim HK, Park DS, Kim JH, Yoon TR. Inhibition of JNK and ERK pathways by SP600125-and U0126-enhanced osteogenic differentiation of bone marrow stromal cells. J Tissue Eng Regen Med. 2012;9(6):283–94.
29. Higuchi C, Myoui A, Hashimoto N, et al. Continuous inhibition of MAPK signaling promotes the early osteoblastic differentiation and mineralization of the extracellular matrix. J Bone Miner Res. 2002; 17(10):1785–94.

30. Kolanczyk M, Kossler N, Kuhnisch J, et al. Multiple roles for neurofibromin in skeletal development and growth. Hum Mol Genet. 2007;16(8):874–86.
31. Stevens DM, Gilmore KA, Harth E. An assessment of nanosponges for intravenous and oral drug delivery of BCS class IV drugs: drug delivery kinetics and solubilization. Polymer Chem. 2014;5:3551–4.
32. Elefteriou F, Benson MD, Sowa H, et al. ATF4 mediation of NF1 functions in osteoblast reveals a nutritional basis for congenital skeletal dysplasiae. Cell Metab. 2006;4(6):441–51.
33. Tsuji K, Cox K, Bandyopadhyay A, Harfe BD, Tabin CJ, Rosen V. BMP4 is dispensable for skeletogenesis and fracture-healing in the limb. J Bone Joint Surg Am. 2008;90(Suppl 1):14–8.
34. Alam N, St-Arnaud R, Lauzier D, Rosen V, Hamdy RC. Are endogenous BMPs necessary for bone healing during distraction osteogenesis? Clin Orthop Relat Res. 2009;467(12): 3190–8.
35. Tang Y, Wu X, Lei W, et al. TGF-beta1-induced migration of bone mesenchymal stem cells couples bone resorption with formation. Nat Med. 2009;15(7):757–65.
36. Birke O, Schindeler A, Ramachandran M, et al. Preliminary experience with the combined use of recombinant bone morphogenetic protein and bisphosphonates in the treatment of congenital pseudarthrosis of the tibia. J Child Orthop. 2010;4(6):507–17.